Ultrafast High-Temperature Sintering (UHS) of Ti and TiNb alloys

Izabeli Ferrari Libraga[1], Angelica Daiane Schneider[2], Martin Bram[3], Natália de Freitas Daudt[1*]

[1]Mechanical Engineering Post-Graduate Program (PGMEC), Universidade Federal de Santa Maria, 97105-900 Santa Maria, RS, Brazil

[2]Physics Post-Graduate Program (PPGFísica), Universidade Federal de Santa Maria, 97105-900 Santa Maria, RS, Brazil

[3] Institute of Energy and Climate Research (IEK-1), Forschungszentrum Jülich GmbH, 52425 Jülich, Germany

[*]Corresponding author: natalia.daudt@ufsm.br

Abstract

Ultra-high temperature sintering (UHS) is an innovative process that rapidly heats materials, allowing for high densification and phase transformation within seconds. Initially developed for ceramics, fundamental research has been started recently to apply UHS for rapid sintering of metals as well. This study explores the UHS sintering of titanium and the titanium niobium alloy (Ti-20Nb) starting from elemental powders. The effects of UHS current and dwell time on the microstructure, phase composition and hardness were analyzed. A densification up to 85% was achieved within a sintering time of only 120 seconds. The formation of β phase was observed in Ti-20Nb parts. As expected, the amount of β phase increased with higher current and dwell time caused by the accelerated interdiffusion of Ti and Nb. Furthermore, a thin titanium carbide layer was formed on the surface of Ti and Ti-20Nb parts due to carbon diffusion from the carbon felt used during UHS. This layer could be removed by surface polishing. The study demonstrates that UHS can densify Ti and TiNb parts in seconds, yielding microstructural characteristics similar to those produced by conventional sintering methods. UHS shows promise for rapid sintering in additive manufacturing of titanium, potentially speeding up the development and production of metals alloys.

Keywords: sintering, powder metallurgy, titanium alloys, Ultrafast High-temperature sintering (UHS)

1. Introduction

Titanium and its alloys have garnered significant attention due to their remarkable combination of high specific strength, low density, and good corrosion and creep resistance. Microstructure and mechanical properties of titanium alloys can vary significantly with the addition of alloying elements, thereby enabling a wide range of applications [1, 2]. For instance, adding niobium enhances biocompatibility, making titanium-niobium alloys highly promising for biomedical implants [3].

The machinability of titanium and its alloys is generally considered poor due to their low thermal conductivity, high chemical reactivity, and low modulus of elasticity. The combination of high cutting temperatures and extensive tool wear poses significant challenges in machining, resulting in high production and machining costs [4]. Powder metallurgy presents a solution to these challenges, enabling the manufacturing of titanium alloys with more intricate geometries [5, 6]. In powder metallurgy – similar to ceramic's fabrication – a sintering step is applied to consolidate loose powders into a bulk solid. This step involves heating the material below its melting temperature, allowing particles to bond without melting by solid state diffusion, thus creating a bulk material with exceptional properties. In traditional sintering methods, temperature and heating duration are the key parameters for achieving densification and grain growth during sintering. However, there is a growing demand for energy-efficient processes, driving the need to lower sintering temperatures and reduce heating times [7].

Over the last decades, several efforts were reported focusing on developing electromagnetic field-assisted sintering techniques to shorten the sintering cycle times and facilitating manufacturing more complex geometries [8]. In 2020, Wang et al. developed a new technique to sinter ceramics named Ultrafast High-Temperature Sintering (UHS). This technique enables to achieve heating rates up to 10^4 °C/min and reduce sintering time to seconds by placing the pre-compacted sample in a carbon felt, which is heated by the Joule effect using an external power source. As a demonstration of the process, Wang et al. synthesized amongst others Ta-doped $Li_{6.5}La_3Zr_{1.5}Ta_{0.5}O_{12}$ (LLZTO), a garnet-type ceramic. In the UHS method, the LLZTO precursors rapidly reacted and densified in about 40 s, 30 s for the heating ramp and 10 s for isothermal sintering at 1500 °C. This resulted in a high density of ~ 97% and relatively small grain sizes compared to those of LLZTO garnets sintered in a conventional resistive furnace [9].

Mishra et al. [10] investigated the densification and grain growth behavior of strontium titanate sintered by UHS, using exceptionally high heating rate of 10^4 °C/min, maximum current ranging from 16 A to 24 A and a constant dwell time of 10 s. However, due to these high heating rates, precise temperature measurements of the samples were unattainable. The study revealed that by regulating the current in the graphite heaters the level of densification and microstructure can be tailored. Additionally, the microstructures indicate a different grain growth behavior compared to conventional sintering methods, likely due to changing the activation energy for grain growth. Conversely, high temperatures favor grain boundary and bulk diffusion, leading to rapid densification. However, according to Wang et al. [9] in the case of ultrahigh heating rates of UHS, they bypass the low-temperature region, reducing particle coarsening and maintaining a strong capillary driving force for sintering, similar to other ultrafast heating methods like flash sintering. Therefore, the fast sintering and densification observed in materials produced by the UHS method may arise due to (i) the rapid kinetics resulting from elevated sample temperatures, (ii) an extra chemical driving force that complements the usual capillary driving force for densification through the simultaneous reaction and sintering process, or (iii) the ultrahigh heating rates that enhance densification rates by suppressing the early state of sintering. Recently, Bhandari et al. [11] demonstrated UHS sintering for debinding and sintering of small, net-shaped 3YSZ ceramics parts produced by additive manufacturing

The high densification resulting from this method on ceramic materials inspired its later extension to the sintering of metallic materials. Recently, Wang et al. demonstrated in a preliminary study the UHS sintering of metal parts such as copper, stainless steel and tungsten made from compacts of elemental or pre-alloyed powders [12]. In addition to fast sintering of metals and alloys by solid state diffusion, the high temperatures produced by the carbon heaters also enable to partly melt precursor powders with different melting points, enabling the rapid synthesis of complex alloys. This process efficiently formed expected alloy phases without secondary oxides, as the inert atmosphere and carbon felt prevented oxidation. Furthermore, the authors also stated that the short sintering time prevented carburization from the carbon felt. This proves the UHS technique allows for fast diffusion, liquid phase/reactive sintering at high temperatures, and alloying and consolidation in a single step. This versatile approach can be applied to synthesize and sinter various materials, including pure metals, alloys, and intermetallic compounds. Due to the exceptional adjustability of the sintering temperature in the UHS technique, it becomes possible to synthesize and sinter metals and alloys with diverse melting temperatures. The short sintering duration facilitates the development of multicomponent alloys using elemental powders, avoiding undesired phase segregation. The optimization of sintering temperature and time will enable to tailor material composition and microstructure. This method can offer a universally fast sintering process for powder metallurgy, with the potential to significantly expedite the development of alloy materials and structures. UHS is a promising technology to be combined with sinter based additive manufacturing (AM) methods, it is especially attractive for production of small components like dental or small bone implants.

In the case of titanium alloys, the combination of high reactivity with oxygen coupled with formation of passivating oxide layers and limitations of controlling grain growth and porosity make the sintering process challenging in general. The UHS method presents an alternative approach to sintering metal alloys, achieving high heating rates and short dwell times. Therefore, in the present study, Ultra-fast High temperature Sintering (UHS) of titanium and titanium-niobium alloys made from elemental powders was evaluated. The effects of UHS parameters on the densification of Ti and Ti-20Nb alloy were investigated aiming to contribute to improve the processing of titanium alloys and introduce the UHS method as general sintering route for metal powders.

Materials and Methods

As starting materials, titanium (particle size 16 - 41 µm) and niobium (particle size 15 – 45 µm) elemental powders supplied by Shijiazhuang Runlong Filter Materials and H.C. Starck Ampertec, respectively, were employed. Ti parts were composed of 100 wt.% Ti powder and the Ti-20Nb parts were composed of 80 wt.% Ti powder and 20 wt.% Nb powder. Green parts were produced by cold compaction for that the powders were mixed with mortar and pestle manually and added to a die of 8 mm diameter – the amount of powder was adjusted to obtain green samples of about 1.3 mm height – then the samples were compacted by applying a uniaxial pressure of 300 MPa. An average green density of 3.2 g·cm^{-3} (71 % of theoretical density) and 3.7 g·cm^{-3} (69 % of theoretical density) were achieved in the Ti and Ti-20Nb parts, respectively.

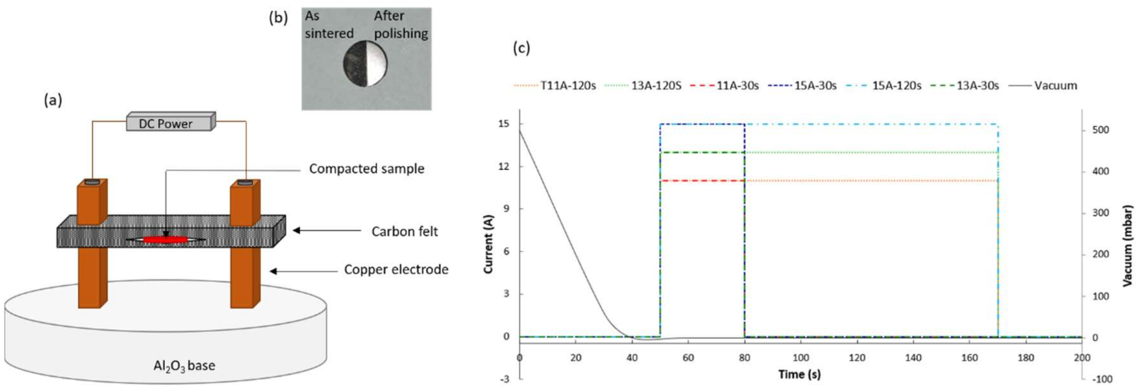

Figure 1. Schematic sketch of Ultrafast High-temperature Sintering setup (a), photograph of UHS sintered Ti part before and after polishing (b) and electric current and vacuum profile of the UHS cycle at 4 different maximum currents (c).

A custom-made UHS set-up (Figure 1 a) placed in vacuum chamber was used for sintering experiments as described elsewhere [10]. The samples were placed in a slice cut in the middle of the carbon felt (size 80 x 9.5 x 4 mm^3) and then fixed into the UHS device. After the mild vacuum was achieved (< 0.2 mbar), the direct electric current (11, 13, and 15A) was applied to the carbon felt using AC/DC power source (TruPlasma Bipolar Series 4000, Trumpf Hüttinger). After the maximum current was achieved, it was held for 30 or 120 seconds to sinter the samples mostly through radiative heat transfer and the power source was switched off as shown in Figure 1 b. These current and dwell times were selected to obtain temperatures in the range 1200 – 1500 ºC based on temperature model developed for this UHS set up and published elsewhere [10]. Due to the very high heating rates, the sample temperature itself could not be measured adequately.

Table 1 summarizes the UHS parameters applied in this study as well as interstitial contents of starting powders and UHS samples.

Table 1 . UHS sintering parameters and interstitial uptake after UHS. Interstitial contents of starting powders are given as reference.

Sample	Maximum current (A)	Dwell time (s)	Carbon Content (wt.)	Oxygen Content (wt.)
Ti powder	-	-	0.013	0.385
Nb powder	-	-	<0.001	0.157
Ti-11-30	11	30	0.877	0.737
Ti-11-120	11	120	0.590	1.28
Ti-13-30	13	30	0.367	0.823
Ti-13-120	13	120	0.702	1.04
Ti-15-30	15	30	0.373	0.859
Ti-15-120	15	120	0.663	1.39
Ti20Nb-11-30	11	30	0.895	0.966
Ti20Nb-11-120	11	120	0.488	1.18
Ti20Nb-13-30	13	30	0.504	0.991
Ti20Nb-13-120	13	120	0.793	1.07
Ti20Nb-15-30	15	30	0.451	0.853
Ti20Nb-15-120	15	120	0.815	1.45

Scanning electron/energy dispersive x-ray spectroscopy (SEM/EDS) analysis was performed to analyze Ti and Nb interdiffusion, densification and grain size. For that, the cross sections of the samples were metallographically prepared and examined by light microscopy (B201, Olympus) and scanning electron microscopy (JSM 6360, Jeol). Energy Dispersive Spectroscopy (EDS) analysis was performed using a Quantax 75 (Bruker Nano GmbH). Archimedes method using a precision balance (EMB, Kern) equipped with a floating device and image analysis of light microscopy images was performed to investigate the porosity. Phase composition was analyzed by X-Ray diffraction using Cu Kα radiation in a Bruker AXS, D8 Advance diffractometer, XRD measurements were performed before and after surface polishing. Hardness was evaluated using a Shimadzu HMV microhardness tester applying a load of 4.90 N for 15 s, following the ASTM E384-05a [13]. The uptake of interstitial elements (oxygen and carbon) of starting powders and sintered parts was evaluated by IR spectroscopy using a TCH/CS 600 equipment (LECO Corp., St Joseph, USA).

Results and Discussion

Ti and TiNb samples were sintered by UHS at different currents (11, 13 and 15 A) and dwell times (30 and 120 s) as shown Figure 2. The Ti samples sintered at 15 A and 120 s melted which suggested that the temperature exceeded 1648 ºC (titanium carbon eutectic melting point) as shown in Figure 2. The Ti-20Nb samples sintered at 15 A and 120 s tend to show onset of partial melting as well as indicated by the color change at the edge. The samples showed a nonmetallic blackish surface indicating there was carbon diffusion from the carbon felt to the samples surface during sintering. However, this layer could be easily removed by polishing as shown in Figure 1b. XRD pattern in the as-sintered state also indicated that a titanium carbide (Ti_2C, and TiC) layer was formed during sintering and that this layer could be removed after polishing (Figure 1 b, Figure 3). Furthermore, in Figure 3 it is possible to notice a displacement to the left of diffraction peaks identified as Ti-α (JCPDS – 00-005-0682) after UHS sintering, which can be related to changes in d-spacing, dislocation densities or residual stress. As UHS involves a high thermal gradient, residual stress is expected to be formed due to rapid heating/ cooling rates as observed in other process of titanium alloys which involve high thermal gradients such as quenching [14] and laser powder bed fusion [15].

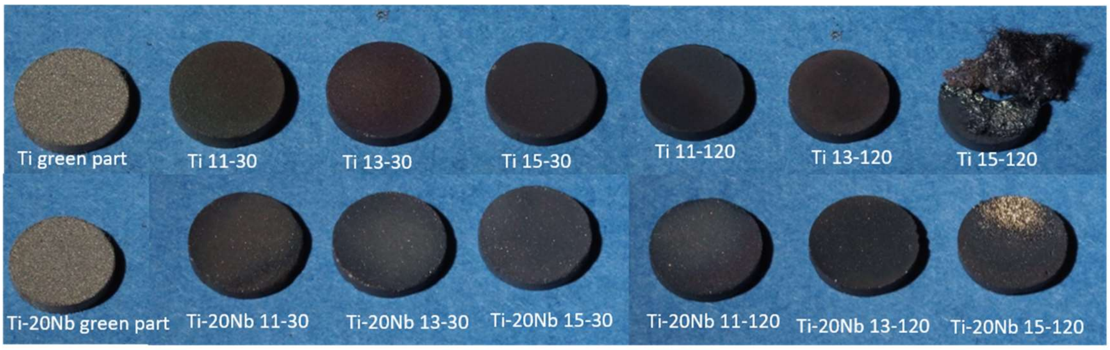

Figure 2. Photographs of green compacts and UHS sintered parts at different maximum currents and dwell times.

The interstitial content of Ti and Ti-20Nb parts sintered by UHS is shown in Table 1. The interstitial content significantly increased compared to starting powders and it is considerable higher than interstitial uptake of Ti-Nb sintered in vacuum furnace [16]. These results indicated that in the case of UHS of alloys with high affinity to oxygen and carbon such as Ti alloys, it is required to mitigate carbon diffusion from carbon felt and oxygen uptake. Some options could be the use of a protection layer such as BN plates reported by Zhang et al. for sintering LLZO [17], or the use of another heater material such as tungsten [18].

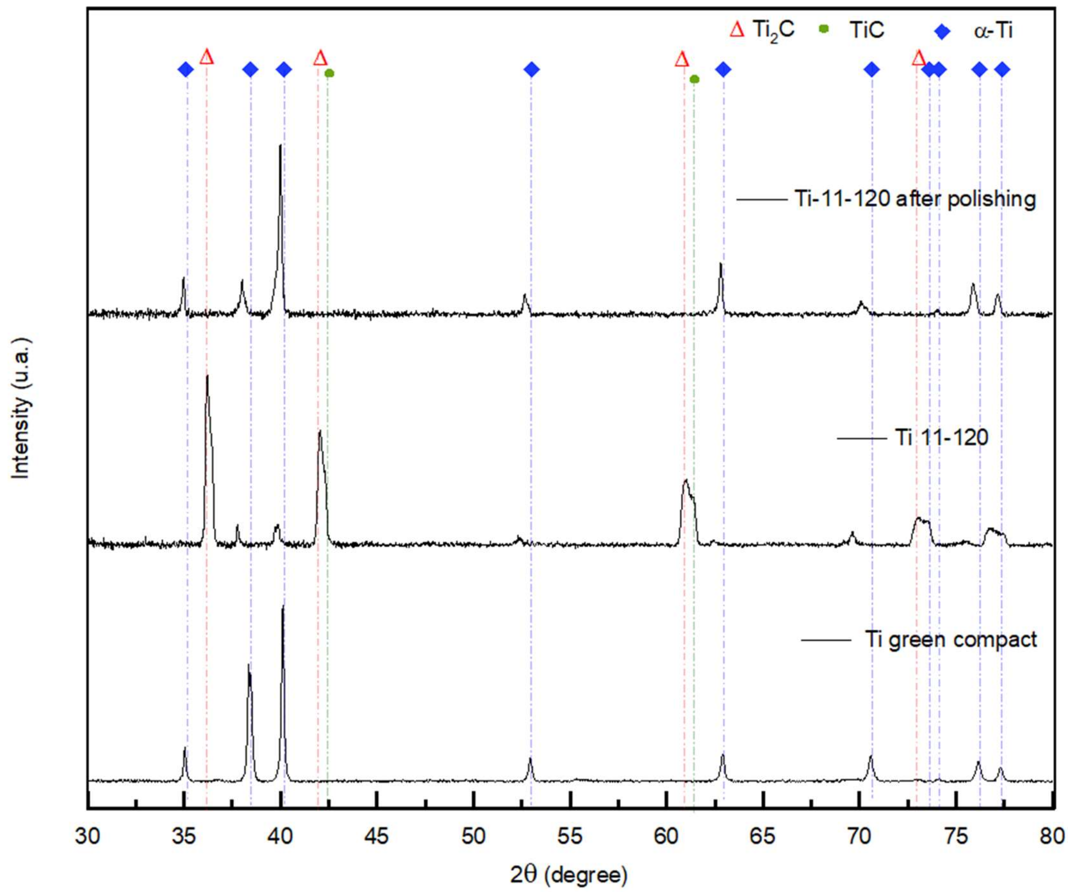

Figure 3. XRD pattern of green Ti part (a) and Ti part sintered by UHS at 11 s for 120 s before (b) and after (c) polishing.

In the Ti samples, the highest relative density of 85 % was found in the samples sintered at 15 A for 30 s. The density increased as function of maximum current and dwell time. However, the Ti samples sintered at 15 A for 120 s melted as shown in Figure 2, therefore the density of the Ti-15-120 samples was not measured. In the Ti-20 Nb samples, the same behavior was observed: the density increased as function of maximum current and dwell time, whereas the highest density was observed in the samples sintered at 15 A for 120 s.

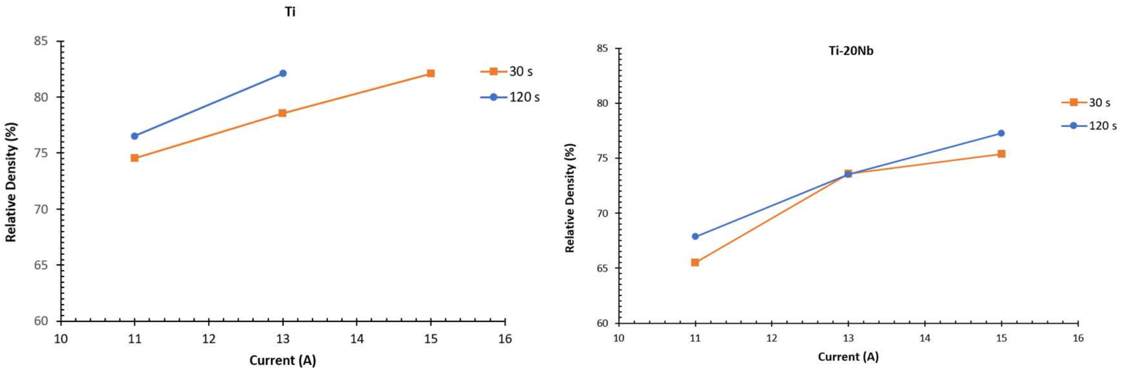

(a) (b)

Figure 4. Relative density as function of maximum current hold by 30 s and 120 s (a) Ti samples and (b) Ti-20Nb samples.

Ti parts sintered by UHS consist of α-Ti microstructure with mainly closed porosity indicating that a final stage of sintering was achieved, as shown in the micrograph of Ti samples (Figure 5). The microstructures indicated that with increasing current and dwell time the porosity decreased, in line with the density values measured by the Archimedes method (Figure 4 a). This behavior is consistent with the idea that a higher sintering temperature, in this case, achieved by using a higher current and longer dwell time, increases sample densification. The possibility of producing homogenous porous structures and net-shaped parts [Reference 11] can make this technology attractive for manufacturing of bone implants and may potentially attract more attention for the commercial use of this method in the future.

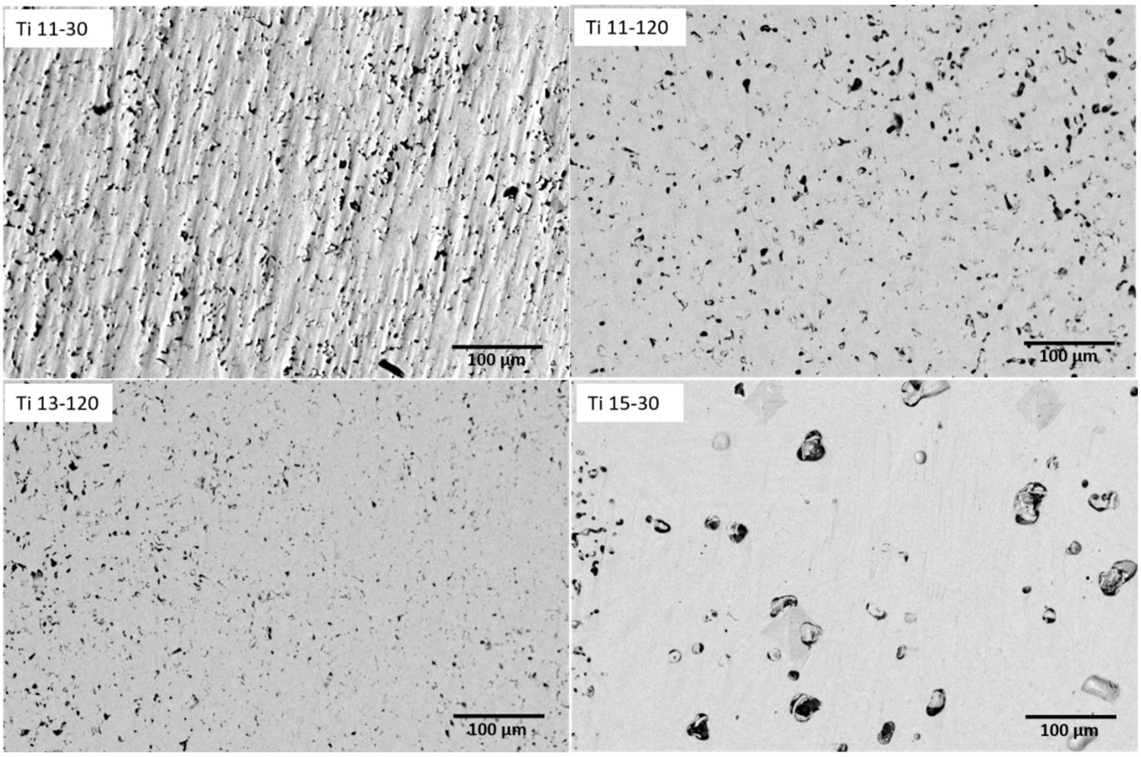

Figure 5. SEM images of Ti parts sintered by UHS: Ti 11-30, Ti11-120, Ti13-120 and Ti15-30 parts.

The microstructure of Ti-20Nb parts sintered at 11A for 30 s mainly consist of the original α-Ti grains and Nb grains, while the microstructure of the other Ti-20Nb parts (sintered at 11A for 120 and the part sintered at 13 and 15 A for 30s and 120 s) consists of (α+β) microstructure with residual Nb grains (Figure 6). As expected, the amount of Nb grains decreases with increasing current and dwell time, which can be related to increased interdiffusion between Nb and Ti grains achieved at higher temperature. The EDS compositional maps of Ti-20Nb shown in Figure 7 also indicated the clearly pronounced interdiffusion of Ti and Nb particles, which improved with increasing sintering temperature (achieved by increasing current and dwell time). It can also be noticed that diffusion of Nb atoms in β-Ti is much higher than the diffusion of Ti atoms in Nb, which result in a Kirkendall porosity in Ti-Nb interface as reported by Zhao et al. [19] and Santos et al. [20] in the conventional sintering of TiNb parts. In the case of longer dwell times, a higher interdiffusion was achieved, so that the Ti-20Nb 15-120 and Ti-20Nb 13-120 parts have better homogenization with a small amount of residual Nb grains and larger pore size, the latter probably due to a stronger pronounced Kirkendall effect.

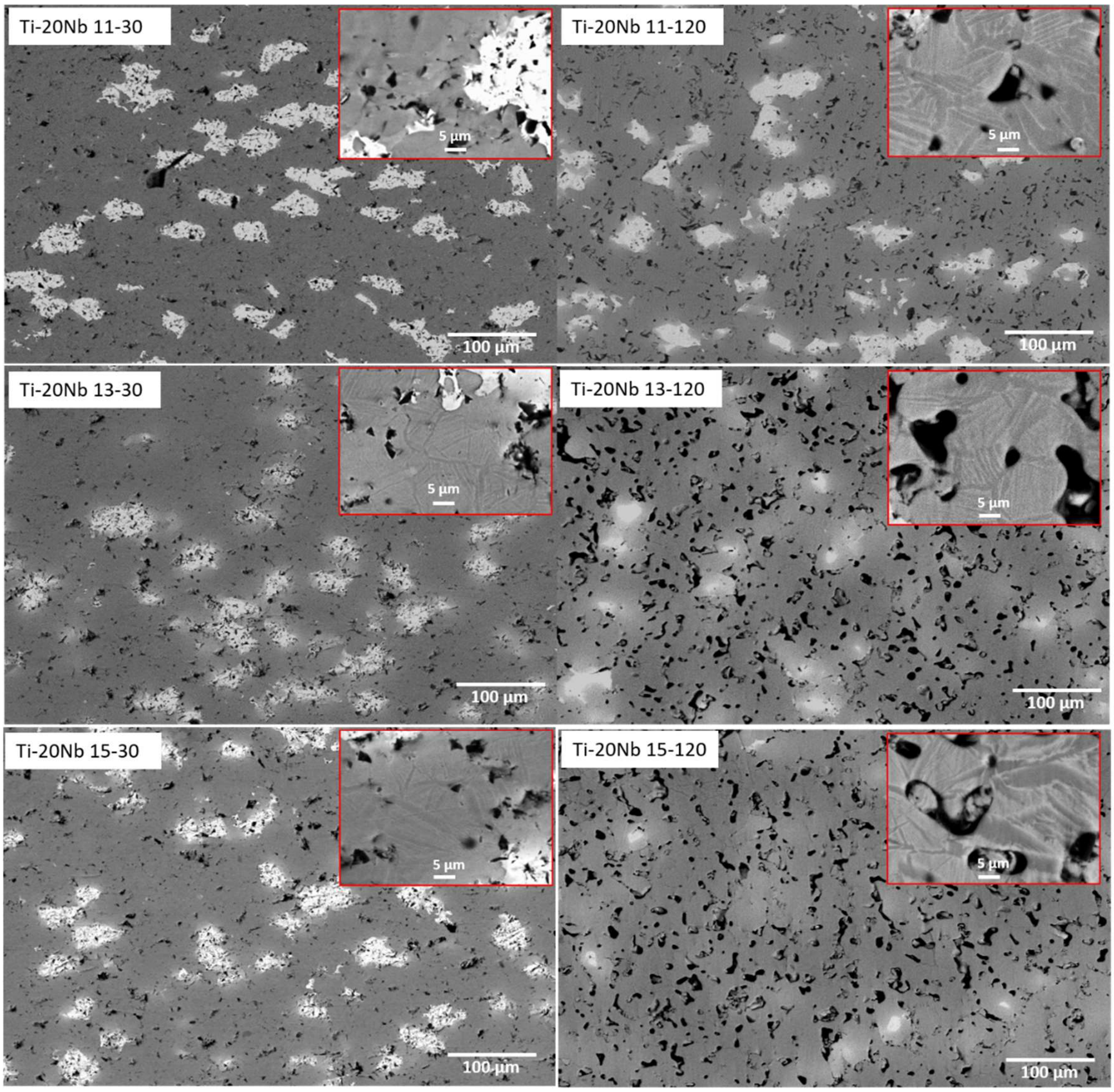

Figure 6. SEM images of Ti-20Nb parts sintered by UHS: Ti-20 11-30, Ti-20Nb 11-120, Ti-20Nb 13-30, 13-120 and Ti15-30 parts.

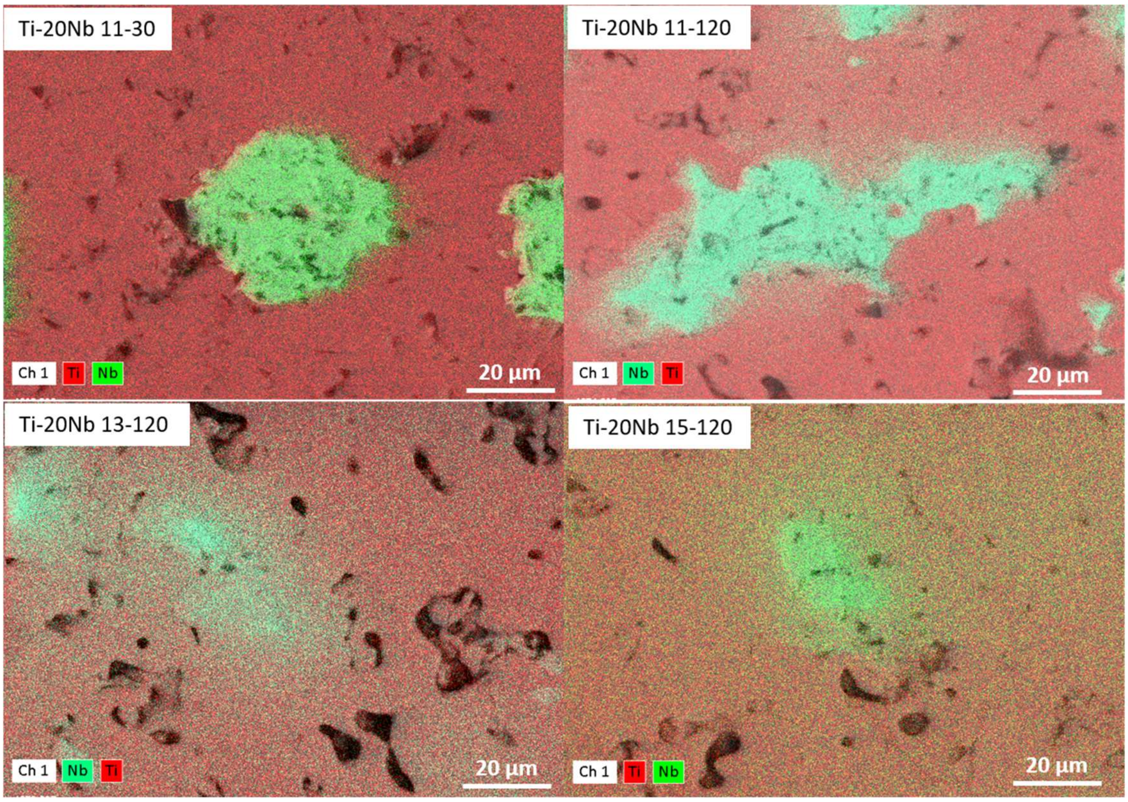

Figure 7. EDS compositional map of Ti-20Nb parts sintered by UHS.

At higher temperatures, Nb and Ti interdiffusion is enhanced and as consequence the β-Ti stability is increased, resulting in higher amount of β-Ti phase as suggested by the XRD pattern shown in Figure 8. During cooling, an increased β-Ti stability can slow down the β/α transformation potentially leading to distortion in the lattice paraments of α-Ti, evidenced by the displacement of α-Ti peaks. No carbides were observed in XRD pattern of Ti-20Nb parts after their surfaces were polished.

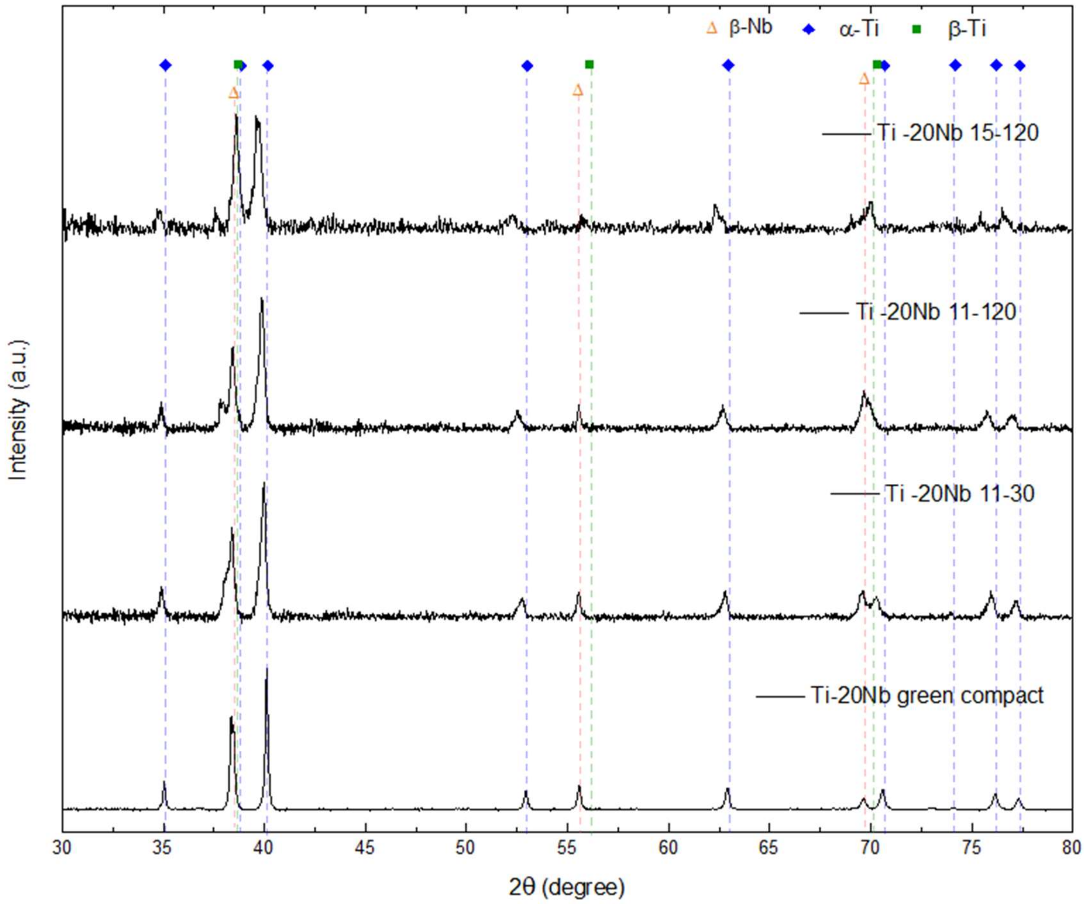

Figure 8. XRD patterns of Ti-20Nb parts before sintering and after sintering by UHS at 11 A for 30 s, 11 for 120 s, 15 for 120 s parameters (sintered samples were polished prior the XRD analysis).

Analyzing hardness measurements of titanium samples after polishing (Figure 9 a), a trend of increasing average hardness is observed in samples with higher sintering current while keeping the sintering time constant. The same behavior of an increase in average hardness is also observed with an increase in sintering time while keeping the sintering current constant. This indicates that – as expected – the more densely sintered samples, associated with higher sintering temperatures, exhibit higher hardness results.

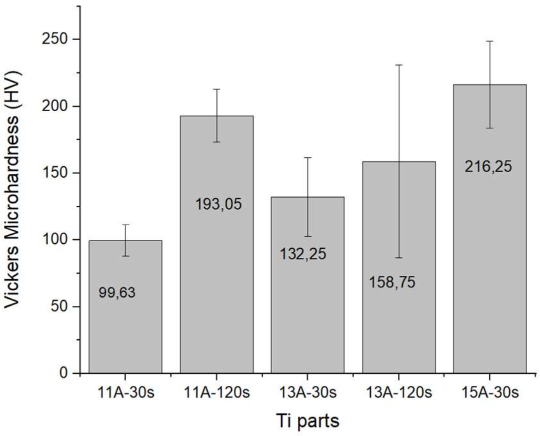

(a)

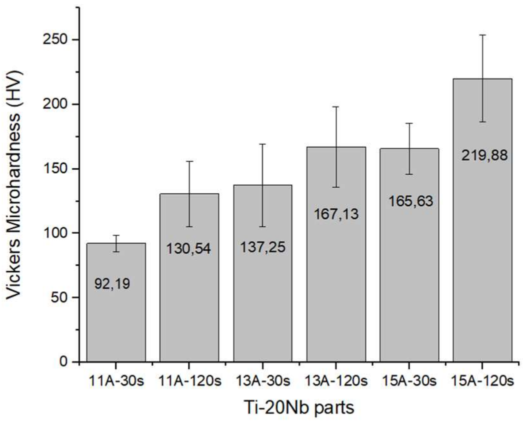

(b)

Figure 9. Microhardness of (a) Ti samples and (b) Ti-20Nb samples.

Analyzing hardness measurements of titanium-niobium parts (Figure 9 b), there is an upward trend in the alloy's average hardness with an increase in sintering current while keeping the sintering time constant. And same behavior was observed, for an increase in sintering time while maintaining a constant current. This can be explained by the reduction of porosity in spite of larger pore size and increased dissolution of niobium in samples sintered for a longer duration, as observed in SEM and EDS analyses, the high Nb dissolution leads to the solid solution strengthening of the α-Ti phase [21, 22].

Conclusions

Sintering of titanium and titanium-niobium alloys in a matter of seconds using the UHS method was successfully demonstrated. From our results, the following conclusions drawn:

- UHS enabled to produce Ti and Ti-20Nb parts with density up to 85 % in just 120 s.
- After sintering samples showed a thin carbide layer which could be easily removed by polishing.
- Ti parts show a homogeneous α-Ti microstructure, while Ti-20Nb parts are composed of α + β microstructure with some residual Nb grains.
- As expected, the amount of residual Nb grains was decreased with increasing current and dwell time during UHS sintering of Ti-20Nb parts.

- Both Ti and Ti-20Nb parts achieved a final stage of sintering still with a considerable amount of residual pores (15-32 vol.%). The possibility of producing homogenous porous structures can make this technology attractive for manufacturing of bone implants.
- Further optimization of UHS experimental setup and parameters are required to achieve higher densification and decrease of interstitial uptakes, e.g., by applying protective coatings or non-graphite heating elements.
- UHS is a promising method for densifying metal alloys in a matter of seconds, producing microstructural characteristics similar to those resulting from conventional sintering methods.

Acknowledgements

Experimental support of Ralf Steinert and Dr. Luca Balice (UHS sintering) as well as Sigrid Schwartz-Lückge (Archimedes method), all at Forschungszentrum Jülich, is highly acknowledged.

References

[1] M. Niinomi, "Mechanical properties of biomedical titanium alloys," *Materials Science and Engineering: A,* vol. 243, pp. 231-236, 1998.

[2] K.E. Agbovi, B. Girault, J. Fajoui, S. Kabra, W. Kockelmann, P.A. Dubos, D. Gloaguen, "Effect of Temperature on the Lattice Strain Evolution in a Textured Alpha Titanium: Neutron Diffraction and Modelling," *JOM,* p. 3055–3066, 2023.

[3] R. Karre, M. K. Niranjan, S. R. Dey, "First principles theoretical investigations of low Young's modulus beta Ti–Nb and Ti–Nb–Zr alloys compositions for biomedical applications," *Materials Science and Engineering: C,* vol. 50, pp. 52-58, 2015.

[4] X. Yang, C. R. Liu, "Machining titanium and its alloys," *Machining Science and Technology ,* vol. 3, no. 1, pp. 107-139 , 1999.

[5] Z. Z. Fang, J. D. Paramore, P. Sun, K. S. R. Chandran, Y. Zhang, Y. Xia, F. Cao, M. Koopman, M. Free, "Powder metallurgy of titanium–past, present, and future," *International Materials Reviews,* vol. 63, no. 7, pp. 407-459, 2018.

[6] L. Guo, F. Yang, B. Lu, C. Zhang, C. Chen, Z. Guo , " Microstructure Evolution and Strength Mechanism of Metastable Powder Metallurgy Ti-6554 Titanium Alloys Under Different Heat Treatment Conditions," *JOM,* vol. 75, p. 2497–2510, 2023.

[7] M. Biesuz, S. Grasso, V. M. Sglavo , "Whats new in ceramics sintering? a short report on the latest trends and future prospects," *Current Opinion in Solid State and Materials Science ,* vol. 24, no. 5, p. 100868, 2020.

[8] M. Kermani, C. Hu, S. Grasso, "From pit fire to ultrafast high-temperature sintering (uhs): A review on ultrarapid consolidation," *Ceramics International,* vol. 3, no. 1, pp. 4017-4029, 2023.

[9] C. Wang, W. Ping, Q. Bai, H. Cui, R. Hensleigh, R. Wang, A. H. Brozena, Z. Xu, J. Dai, Y. Pei et al., "A general method to synthesize and sinter bulk ceramics in seconds," *Science,* vol. 368, no. 6490, pp. 521-526, 2020.

[10] T. P. Mishra, S. Wang, C. Lenser, D. Jennings, M. Kindelmann, W. Rheinheimer, C. Broeckmann, M. Bram, O. Guillon, "Ultra-fast high-temperature sintering of strontium titanate," *Acta Materialia,* vol. 231, p. 117918, 2022.

[11] S. Bhandari, C. Manière, F. Sedona, E. De Bona, V. M. Sglavo, P. Colombo, L. Fambri, M. Biesuz, G. Franchi, "Ultra-rapid debinding and sintering of additively manufactured ceramics by ultrafast high-temperature sintering," *Journal of the European Ceramic Society,* vol. 44, no. 1, pp. 328-340, 2024.

[12] C. Wang, W. Zhong, W. Ping, Z. Lin, R. Wang, J. Dai, M. Guo, W. Xiong, J.C. Zhao,L. Hu, "Rapid Synthesis and Sintering of Metals from Powders," *Advanced Science,* vol. 8, no. 12, p. 2004229, 2021.

[13] ASTM: American Society for Testing and Materials, "ASTM E9: standard test methods of compression testing of metallic materials at room temperature.," *West Conshohocken: ASTM International,* 2009.

[14] J. Teixeira, D. Maréchal, R.C. Wimpory, S. Denis, F. Lefebvre, R. Frappier , "Formation of residual stresses during quenching of Ti17 and Ti–6Al–4V alloys: Influence of phase transformations," *Materials Science and Engineering: A,* vol. 832, p. 142456, 2022.

[15] X. Chen, X. Xie, H. Wu a, X. Ji, H. Shen, M. Xue, H. Wu,, "In-situ control of residual stress and its distribution in a titanium alloy additively manufactured by laser powder bed fusion," *Materials Characterization ,* vol. 201, p. 112953, 2023.

[16] N. F. Daudt, F.J. Hackemüller, M. Bram, "Manufacturing of Ti-10Nb based metal sheets by tape casting," *Materials Letters,* vol. 237, pp. 161-164, 2019, ~~Pages~~ .

[17] H. Zhang, R. Dubey, M. Inniger, F. Okur, R. Wullich, "Ultrafast-sintered self-standing LLZO membranes for high energy density lithium garnet," *Cell Reports Physical Science,* vol. 4, p. 101473, 2023.

[18] J. Wu, M. Kermani, D. Zhu , J. Li, Y. Lin, C. Hu, S. Grasso, "Carbon free ultra-fast high temperature sintering of translucent zirconia," *Scripta Materialia ,* vol. 210, p. 114476, 2022.

[19] D. Zhao, K. Chang, T. Ebel, H. Nie, R. Willumeit, F. Pyczak, "Sintering behavior and mechanical properties of a metal injection molded Ti–Nb binary alloy as biomaterial," *Journal of Alloys and Compounds,* vol. 640, p. 393–400, 2015.

[20] D. M. C. dos Santos, F. Signor, A.D. Schneiderb, C. R. Benderc, P. H. Marezea, N.F. Daudt, "Powder Metallurgical Manufacturing of Ti-Nb alloys Using Coarse Nb Powders," *Materials Research,* vol. 27, p. e20230478, 2024.

[21] C. M. Lee, C. P. Ju, J. H. Chern Lin, "Structure-property relationship of cast Ti-Nb alloys," *J Oral Rehabil,* vol. 29, no. 4, pp. 314-22, 2002.

[22] ~~D. M. C. dos Santos, F. Signor, A.D. Schneider, C. R. Bender, P. H. Mareze , N.F. Daudt, "Powder Metallurgical Manufacturing of Ti-Nb alloys Using Coarse Nb Powders," *Materials Research,* vol. 27, p. e20230478, 2024.~~